Proceedings of the 17th World Congress
The International Federation of Automatic Control
Seoul, Korea, July 6-11, 2008

Stability Crossing Surfaces for Systems with Three Delays

Elham Almodaresi and Mohammad Bozorg

Dept. of Mechanical Engineering, Yazd University
P.O. Box 89195-741, Yazd, Iran.

Abstract: The stability of linear time-delay systems whose characteristic equations include three delays is investigated. Using geometrical relations in the polynomial plane, a graphical method is presented to visualize the stability domains in the three-dimensional space of time delays. Also, in this space, the surfaces on which the number of unstable poles of the system changes, are identified and an algorithm is presented to plot these surfaces. This work extends the results of previous works on the plane of two delays, to the three-dimensional case and initiates new studies in this direction.

1. INTRODUCTION

In many time-delay systems, the delays are not fixed and vary in some ranges. For such systems, it is desirable to compute the permissible ranges of delays to maintain stability. Robustness of time-delay systems with respect to delay perturbations, has been subject of many research efforts (see Niculescu, 2001; Gu, *et al*., 2003; Zhong, 2006).

For linear systems characterized by linear delay-differential equation

$$\sum_{i=0}^{m}\sum_{k=0}^{n} p_{ik}\frac{d^k x(t-\tau_i)}{dt^k}=0, \tag{1}$$

where the coefficients p_{ik}, $i=0,1\text{K}\ ,m$, $k=0,1,\text{K}\ n$ are real numbers, $\tau_0=0$ and $\tau_i>0$, $i=1,\text{K}\ ,m$ are time-delays, the characteristic quasipolynomial

$$p(s,\boldsymbol{\tau})=p_0(s)+p_1(s)e^{-\tau_1 s}+\Lambda\ +p_m(s)e^{-\tau_m s}, \tag{2}$$

where

$$p_i(s)=\sum_{k=0}^{n} p_{ik}s^k\ , p_{0n}\neq 0, \tag{3}$$

determines the stability of the system (Gu, *et al*., 2005). While in Gu *et al*. (2005), the two-delay case (m=2) was considered, here the more general case of three delays (m=3) is investigated.

Time-delay systems of form (1) can be divided into two categories of *neutral* and *retarded* systems, corresponding respectively to the cases of inclusion or exclusion of delay in the highest order of the derivatives. Also, when the time delays $\tau_0,\text{K}\ ,\tau_m$ are the multiples of a constant, the delays are called "commensurate" delays. For a thorough review of the results on various time delay systems, see Richard (2003).

For systems with commensurate delays, allowable margins of delay perturbation to maintain stability were computed in Barnett (1983), Walton and Marshall (1987) and Chiasson (1988). In Rekasius (1980), using the bilinear transformation, the quasipolynomials are transformed into polynomials. Olgac and Sipahi (2002) use this technique to compute the delay perturbation margin for retarded systems. Barmish and Shi (1989) and Chen *et al.* (1995) use frequency search methods to compute this margin.

For systems with incommensurate delays, Sipahi and Olgac (2004, 2005) compute the stability domains for retarded systems with two delays and a linear combination of two delays. A frequency sweeping method is also presented in Chen and Latchman (1995) to compute the stability borders for retarded systems.

For two-delay systems, in Hale and Huang (1993), a geometrical stability analysis is presented in the time-delay plane. To identify the stability region in this plane, a geometrical method is also presented in Gu, *et al*. (2005). The stability crossing curves are evaluated and different possible shapes of these curves are discussed. For systems with multiple incommensurate delays, few results are available. Among them is the work of Bozorg and Davison (2006), where a numerical method is presented for the computation of the stability radius in the space of multiple time delays.

In this paper, the stability domain of time-delay systems (1) (or (2)) with three delays is computed in the 3*D* space of time delays. The results of Gu *et al*. (2005) are extended to the space of three delays and the stability crossing surfaces are identified in this space. The results are applicable to both neutral and retarded systems. Using the geometrical conditions for forming a quadrangle in the complex plane, the stability crossing curves at different frequencies are computed. This paper is organized as follows. After some preliminary definitions and remarks in Section 2, Section 3 characterizes the frequencies through which the zeros of a quasipolynomial can move to the instability region. Thence, the stability crossing surfaces in the time-delay space are identified in Section 4. Section 5 presents a numerical example and Section 5 concludes the paper.

2. PRELIMINARIES

The characteristic quasipolynomial of a system with three uncertain time-delays is given from (2) as

$$p(s,\boldsymbol{\tau}) = p_0(s) + p_1(s)e^{-\tau_1 s} + p_2(s)e^{-\tau_2 s} + p_3(s)e^{-\tau_3 s}, \quad (4)$$

where $\boldsymbol{\tau} = [\tau_1\ \tau_2\ \tau_3]^T$ denotes a point in the time-delay space, i.e., $\tau \in D \subset \Re_+^3$ where D is the time-delay space and $\Re_+^3$ denotes set of nonnegative real numbers. It is desired to compute the number of unstable zeros of (4) in right half plane (RHP) denoted by C_+, as the set of complex numbers with nonnegative real parts. The following assumptions are made (Gu, *et al*., 2005):

1- Zero frequency assumption:

$$p_0(0) + p_1(0) + p_2(0) + p_3(0) \neq 0 \quad (5)$$

2- Infinite frequency assumption:

$$\lim_{s\to\infty}\left(\left|\frac{p_1(s)}{p_0(s)}\right| + \left|\frac{p_2(s)}{p_0(s)}\right| + \left|\frac{p_3(s)}{p_0(s)}\right|\right) < 1 \quad (6)$$

The following Lemma can be stated from Gu *et al*. (2005), as only a new dimension is added to the problem and assumptions (5) and (6) are made.

Lemma 1. As $\boldsymbol{\tau}$ continuously varies within $\Re_+^3$, the number of zeros of $p(s,\ \boldsymbol{\tau})$ on C_+ can change only if a zero crosses the imaginary axis.

Remark 1. The result of Lemma 1 can be considered as a counterpart to the parameter space results of Ackermann (2002) for polynomials. The stability crossing boundaries can be categorized as:

1) *Real Root Boundary* (RRB), which corresponds to the zero frequency crossing points, according to (5),

2) *Infinite Root Boundary* (IRB), which corresponds to the zero frequency crossing points, according to (6),

3) *Complex Root Boundary* (CRB), which corresponds to the zero frequency crossing points on the imaginary axis, which is addressed by Lemma 1.

Remark 2. The domains in the time-delay space $D \subset \Re_+^3$ at which the number of zeros of $p(s,\boldsymbol{\tau})$ is zero, is the desired stability domain and the crossing points in D at which this number changes, are sought.

3. STABILITY CROSSING FREQUENCIES

In this section, we discuss the frequencies through which the roots of quasipolynomial (4) move to RHP. Let Ω be the set of all frequencies ω>0, at which $p(j\omega,\boldsymbol{\tau}) = 0$ holds. This set, called the "stability crossing frequency set", may include some intervals $\Omega_i = [\omega_i^s, \omega_i^e],\ i = 1,\Lambda\ .N$, where "*s*" stands for "start" and "*e*" stands for "end".

Proposition 1. For each ω>0, $s = j\omega$ can be a solution of (4) at some $\boldsymbol{\tau} \in \Re_+^3$, if and only if

Case a) when $p_0(j\omega) \neq 0$, the bellow inequalities hold:

$$|a_1(j\omega)| + |a_2(j\omega)| + |a_3(j\omega)| - 1 \geq 0, \quad (7\text{-a})$$

$$1 - |a_1(j\omega)| + |a_2(j\omega)| + |a_3(j\omega)| \geq 0, \quad (7\text{-b})$$

$$1 + |a_1(j\omega)| - |a_2(j\omega)| + |a_3(j\omega)| \geq 0, \quad (7\text{-c})$$

$$1 + |a_1(j\omega)| + |a_2(j\omega)| - |a_3(j\omega)| \geq 0, \quad (7\text{-d})$$

where

$$a_i(j\omega) = \frac{p_i(j\omega)}{p_0(j\omega)},\ i = 1,2,3, \quad (8)$$

Case b) when $p_0(j\omega) = 0$ and $p_1(j\omega) \neq 0$, the below inequalities hold:

$$\begin{matrix} |c_1(j\omega)| + |c_2(j\omega)| \geq 1 \\ \big||c_1(j\omega)| - |c_2(j\omega)|\big| < 1 \end{matrix}, \quad (9\text{-a})$$

$$c_i(j\omega) = \frac{p_{i+1}(j\omega)}{p_1(j\omega)}, \quad i = 1,2, \quad (9\text{-b})$$

Case c) when $p_0(j\omega) = p_1(j\omega) = 0,\ p_2(j\omega) \neq 0$ and $p_3(j\omega) \neq 0$, the below equation holds:

$$|p_2(j\omega)| = |p_3(j\omega)|. \quad (10)$$

Proof. Case a) When $p_0(j\omega) \neq 0$, the zeros of (4) are the same as the zeros of the following equation:

$$1 + \sum_{i=1}^{3} a_i(j\omega)e^{-j\tau_i\omega} = 0. \quad (11)$$

Decomposing terms of (11) into magnitudes and phases, one has

$$1 + \sum_{i=1}^{3} |a_i(j\omega)|e^{j\gamma_i} = 0, \quad (12\text{-a})$$

$$\gamma_i = \angle a_i(j\omega) - \tau_i\omega,\ i = 1,2,3\ . \quad (12\text{-b})$$

To satisfy (11), the vector sum of the four terms appearing in the equation must be zero. Therefore, starting from the origin, the vector sum also ends at the origin (Fig. 1).

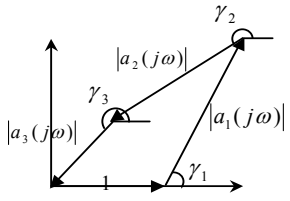

Fig. 1. The quasipolynomial quadrangle.

The necessary and sufficient condition for forming a quadrangle is that the length of each side must be smaller than the sum of the lengths of the other sides, as presented in (7).

Case b) When $p_0(j\omega)=0$ and $p_1(j\omega)\neq 0$, the zeros of (4) are the same as the zeros of the following equation:

$$1+\sum_{i=1}^{2}|c_i(j\omega)|e^{j\gamma_i}=0 \tag{13-a}$$

$$\gamma_i=\angle c_i(j\omega)+(\tau_i-\tau_{i+1})\omega,\ i=1,2 \tag{13-b}$$

In this case, one of the sides of the quadrangle vanishes as $p_0(j\omega)=0$. Then, (13-a) forms a triangle in the complex plane (Fig. 2).

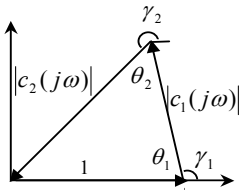

Fig. 2. Triangle form of the quasipolynomial.

Equation (9) presents the necessary and sufficient conditions for forming a triangle.

Case c) When both $p_0(j\omega)$ and $p_1(j\omega)$ vanish, (4) will vanish at $s=j\omega$, if and only if $p_2(j\omega)$ and $p_3(j\omega)$ have the same magnitude and their phase are 180^o apart. □

The Cases b) and c) of Proposition 1 are thoroughly investigated in Gu *et al*. (2005) for two delays, and are not further treated in this paper. Instead, Case a) which is new in this paper and corresponds to the quadrangles of polynomial vectors, is discussed in details.

Let us define the frequencies at which any of (7-a) to (7-d) holds in the equality form as the *root frequencies* $(\omega_r)_j$, $j=1,\mathrm{K}\ ,M$, If these frequencies are ordered, the interval between two successive root frequency can be defined as a frequency interval $\Omega_i=[\omega_i^s,\omega_i^e]$, $i=1,\mathrm{K}\ ,N$, if all $\omega^*\in\Omega_i$ satisfy all (7-a) to (7-d), where ω_i^s and ω_i^e correspond to the root frequencies.

Proposition 2. The number of frequency intervals (*N*) is finite and all the frequencies ω_i^s and ω_i^e, corresponding to the root frequencies, are also finite.

Proof. The root frequencies are the roots of polynomial equations obtained from (7-a) to (7-d) when equalities hold (The absolute values only affect the sign of the polynomials). Since polynomials have a finite number of roots, the number of root frequencies is finite. Also, from assumption (6), if $s=j\omega,\omega\to\infty$, one has $|p_0(j\infty)|>|p_1(j\infty)|+|p_2(j\infty)|+|p_3(j\infty)|$. Multiplying (7-a) to (7-d) by $|p_0(j\omega)|$ and letting $\omega\to\infty$, the dominant terms in the left hand sides will be $|p_0(j\infty)|$. But, this term cannot be zero, since $p_0(j\infty)=p_{0n}(j\infty)^n$ and $p_{0n}\neq 0$. Therefore, $\omega=\infty$ cannot be a root of the left hand sides of (7-a) to (7-d). Therefore, the root frequencies cannot be infinite. □

4. STABILITY CROSSING SURFACES

Define all the points $\tau\in\Re_+^3$ at which $p(s,\boldsymbol{\tau})$ has at least one zero, as the "set of stability crossing surfaces" *S*. This set contains several surfaces formed at different crossing frequencies, as will be shown in this section. We are interested in identifying these surfaces. When $p_0(j\omega)\neq 0$, (7) and (12) characterize the points on *S*. If the arguments $\gamma_1,\gamma_2,$ and γ_3 form a three dimensional space, i.e., $\boldsymbol{\gamma}=[\gamma_1\ \gamma_2\ \gamma_3]^T$, $\boldsymbol{\gamma}\in\Gamma\subset\Re_+^3$, any point $\boldsymbol{\gamma}\in\Gamma$ can be mapped to a point $\boldsymbol{\tau}\in D$ in the time-delay space through the linear transformation (12-b).

Proposition 3. At each root frequency $(\omega_r)_j$, $j=1,\mathrm{K}\ ,M$ (corresponding to ω_i^s *or* ω_i^e), only one point $\boldsymbol{\gamma}\in\Gamma$ with $\gamma_i\in[0,2\pi)$, $i=1,2,3$ satisfies (12-a), but for other crossing frequencies $\omega^*\in(\omega_i^s,\omega_i^e)$, four separate curves in Γ satisfy (12-a).

Proof . From Proposition 1 case a), it is clear that at the limit cases when the equalities hold in (7), the quadrangle deforms to a line and the vectors become collinear. Then, four cases will arise corresponding to the four equations ((7-a) to (7-d)), as shown in Table 1, with each case corresponding to a particular combination of γ_i's.

Table 1. Quadrangle at root frequencies

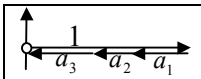	$\gamma_1=\gamma_2=\gamma_3=\pi$	ω_r satisfies (7-a)	Type 1
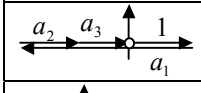	$\gamma_1=\pi$, $\gamma_2=\gamma_3=0$	ω_r satisfies (7-b)	Type 2
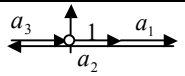	$\gamma_1=0$, $\gamma_2=\pi$, $\gamma_3=0$	ω_r satisfies (7-c)	Type 3
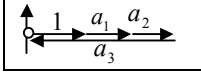	$\gamma_1=\gamma_2=0$, $\gamma_3=\pi$	ω_r satisfies (7-d)	Type 4

For an intermediate frequency $\omega^*\in(\omega_i^s,\omega_i^e)$, more than one combination of $a_i(j\omega^*)$, $i=1,2,3$ can form the quadrangle. To form a quadrangle, as shown in Fig. 3, the locus of the endpoint of the edge a_1 is the circle C_1, centred at the point (1,0) and the radius of $|a_1(j\omega^*)|$, and the locus of the starting point of the edge a_3 is the circle C_3, centred at the origin and the radius of $|a_3(j\omega^*)|$.

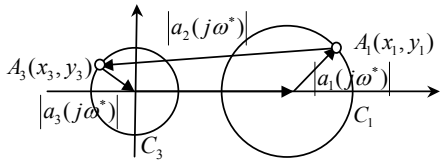

Fig. 3. The geometric relationships of the quadrangle.

To form a quadrangle, one can draw a circle centred at a point $A_1(x_1, y_1)$ on C_1 with the radius $|a_2(j\omega^*)|$ to intersect point $A_3(x_3, y_3)$ on circle C_3. Then, the following equations hold:

$$x_1^2 + y_1^2 = |a_1(j\omega^*)|^2, \tag{14-a}$$

$$(x_3 - x_1)^2 + (y_3 - y_1)^2 = |a_2(j\omega^*)|^2, \tag{14-b}$$

$$x_3^2 + y_3^2 = |a_3(j\omega^*)|^2, \tag{14-c}$$

where

$$x_1 = |a_1(j\omega^*)| \cos\gamma_1 + 1, \tag{15-a}$$

$$y_1 = |a_1(j\omega^*)| \sin\gamma_1, \tag{15-b}$$

$$x_3 = -|a_3(j\omega^*)| \cos\gamma_3, \tag{15-c}$$

$$y_3 = -|a_3(j\omega^*)| \sin\gamma_3. \tag{15-d}$$

By moving A_1 on C_1, its corresponding point A_3 moves on C_3 and the quadrangle deforms continuously. The angles γ_i, i=1,2,3 also vary continuously in the Γ-space, forming a continuous curve.

For given values of $|a_1(j\omega^*)|$, $|a_2(j\omega^*)|$, and $|a_3(j\omega^*)|$, four configurations for the quadrangle can be imagined depending on the selection of the points A_1 and A_3 in up or down half of the circles C_1 and C_3 as shown in Table 2. Therefore, at each ω^*, four curves in the Γ-space are obtained, on which (12-a) holds. □

At each $\omega^* \in (\omega_i^s, \omega_i^e)$, four stability crossing curves are obtained in Γ, and accordingly, in the time-delay space D.

The angles γ_1, γ_2 and γ_3 can be computed as follows:

$$\begin{aligned}\gamma_1 &= \text{atan2}\,(y_1, x_1 - 1),\\ \gamma_2 &= \text{atan2}\,(y_3 - y_1, x_3 - x_1),\\ \gamma_3 &= \text{atan2}\,(-y_3, -x_3),\end{aligned} \tag{16}$$

where atan2(.) is the four quadrant inverse tangent.

From (12-b), these angles can be mapped to the time-delay space via

$$\tau_i = \frac{\angle a_i(j\omega^*) - \gamma_i}{\omega^*}, \quad i = 1,2,3. \tag{17}$$

Table 2. Different forms of the quadrangle

Index	Position of of A_3 on C_3	Position of A_1 on C_1	Quadrangle form
uu	C_1-up	C_3-up	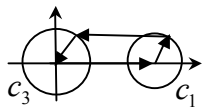
ud	C_1-up	C_3-down	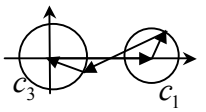
du	C_1-down	C_3-up	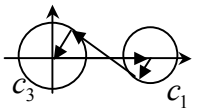
dd	C_1-down	C_3-down	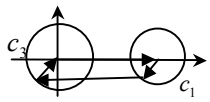

As ω^* is swept in the interval (ω_i^s, ω_i^e), the four curves obtained at each ω^*, continuously move in both Γ and D spaces and form the stability crossing surfaces. It is interesting to note that these surfaces boil down to single points at the two ends of the intervals (ω_i^s and ω_i^e), which correspond to the root frequencies ω_r.

Corollary 1. If for an $\omega^* \in \Omega$, τ^* belongs to the set of stability crossing surfaces S, all the points $[\tau_1^* + (2m\pi/\omega^*)\ \ \tau_2^* + (2n\pi/\omega^*)\ \ \tau_3^* + (2k\pi/\omega^*)]^T$, $m,n,k \in I$ also belong to S.

Corollary 2. From Propositions 2 and 3 and Corollary 1, the set of stability crossing surface S is obtained as

$$S = \left\{ \bigcup_{\omega\in\Omega_i} S_{uu}(m,n,k)) \right\} \cup \left\{ \bigcup_{\omega\in\Omega_i} S_{ud}(m,n,k)) \right\} \cup \left\{ \bigcup_{\omega\in\Omega_i} S_{du}(m,n,k)) \right\} \cup \left\{ \bigcup_{\omega\in\Omega_i} S_{dd}(m,n,k)) \right\},\ m,n,k \in I,\ i = 1,\ldots,N$$

where, S_{uu}, S_{ud}, S_{du}, and S_{dd} denote the four stability crossing curves at each frequency according to Table 2.

Remark 3. (Gu, *et al*., 2005) For the frequencies ω, when $p_0(j\omega) = 0$ and $p_1(j\omega) \neq 0$, (case (b) of Proposition 1) the stability crossing surfaces are the planes

$$\begin{aligned}\tau_2 &= \tau_1 + (\angle c_1(j\omega) - \gamma_1)/\omega,\\ \tau_3 &= \tau_1 + (\angle c_2(j\omega) - \gamma_2)/\omega,\end{aligned} \tag{18}$$

where, depending on the formation of the triangle of Fig. 2 upward (u) or downward (d), γ_1 and γ_2 are computed as

$$\gamma_{1u} = \pi - \theta_1 + 2n\pi,\ \ \gamma_{2u} = 2\pi - \theta_1 - \theta_2 + 2m\pi,\ m,n \in I \tag{19}$$

$$\gamma_{1d} = \pi + \theta_1 + 2n\pi,\ \ \gamma_{2d} = \theta_1 + \theta_2 + 2m\pi,\ m,n \in I \tag{20}$$

and θ_1 and θ_2 are computed from the trigonometry.

Remark 4. (Gu, *et al*., 2005) For the frequencies ω, when $p_0(j\omega) = p_1(j\omega) = 0$, $p_2(j\omega) \neq 0$ and $p_3(j\omega) \neq 0$, (case (c) of Proposition 1), the planes

$$\tau_3 - \tau_2 = (\angle p_3(j\omega) - \angle p_2(j\omega) + 2\pi(n-m) - \pi)/\omega, \quad m,n \in I$$

form the stability crossing surfaces. □

An algorithm for plotting the stability crossing surfaces concludes this section.

Algorithm 1. Plotting Stability Crossing Surfaces

1. Compute the root frequencies (ω_r), $j = 1,\text{K}\,,M$, by calculating the roots of the left hand sides of (7-a) to (7-b).
2. Evaluate the feasible intervals $\Omega_i = [\omega_i^s, \omega_i^e]$, $i = 1,\text{K}\,N$, inside which all inequalities of (7) hold, where ω_i^s and ω_i^e are the root frequencies computed at Step 1. Only a finite frequency range $\Omega = [0, \omega_c]$, where ω_c is a large enough cut-off frequency (see Proposition 2), need to be checked.
3. For the frequencies ω_i^s and ω_i^e, i = 1,…, N compute γ_1, γ_2 and γ_3 from Table 1, and thence τ_1, τ_2 and τ_3 from (12-b) and plot these points in the 3*D* time-delay space.
4. Increment ω^* in each interval (ω_i^s, ω_i^e).
   - 4.1. If ω^* corresponds to the Cases b) and c) of Proposition 1, compute the stability crossing surfaces from Remarks 3 and 4. Otherwise, proceed to 4.2.
   - 4.2. Increment γ_1 in the interval $(0,\pi)$ and $(-\pi,0)$.
     - 4.2.1. Compute x_1 and y_1 from (15-a) and (15-b).
     - 4.2.2. Substitute the computed x_1 and y_1 in (14-b) and (14-c) and solve them for x_3 and y_3. Four sets of solutions will be found at each ω^* according to Table 2.
     - 4.2.3. Compute γ_2 and γ_3 from (16).
     - 4.2.4. Compute $\boldsymbol{\tau}=[\tau_1\ \tau_2\ \tau_3]^{\mathrm{T}}$ from (12-b) and plot this point in the 3*D* time-delay space.
     - 4.2.5. Plot also the points:

       $$[\tau_1^* + (2m\pi/\omega^*)\quad \tau_2^* + (2n\pi/\omega^*)\quad \tau_3^* + (2k\pi/\omega^*)]^T$$

       for feasible values of $m,n,k \in (\ldots,-3,-2,-1,1,2,3,..)$ in the time-delay space. Theoretically, infinite number of surfaces can be obtained, but in practice, there exist some feasible ranges of time delays.

   Loop 4.2

Loop 4

5. EXAMPLE

Consider the quasipolynomial

$$p(s,\boldsymbol{\tau}) = (10s^3 + 4) + (s^3 + 2s + 1)e^{-\tau_1 s} + (4s^2)e^{-\tau_2 s} + (s^2 + 4s + 1)e^{-\tau_3 s}.$$

It is desired to plot the stability crossing surfaces for the quasipolynomial. In particular, the domains in which no unstable root exists (stability domains) are sought. Implementing Algorithm 1, the roots of (7-a) to (7-d) must first be found. Plotting the left-hand side of these equations (Fig. 4) reveals that [0.453, 1.335] is a feasible interval, where all inequalities of (7) hold. At each frequency in this interval, four curves are obtained according to Table 2 (Fig. 5). By sweeping the frequency interval and implementing Step 4 of the algorithm, the stability crossing surfaces are obtained in the τ_1-τ_2-τ_3 space (Fig. 6).

If these surfaces are cut in fixed values of τ_3, several closed stability crossing curves are obtained in the τ_1-τ_2 plane (Fig. 7). To find the stability domains, arbitrary points inside each domain can be checked. The number of unstable zeros (NU) is shown in each domain. This number changes across the stability crossing surfaces. The stability domains are the domains where this number is zero. Interesting materials on the change of number of unstable roots in different directions can be found in Sipahi and Olgac (2004) and Gu *et al*. (2005).

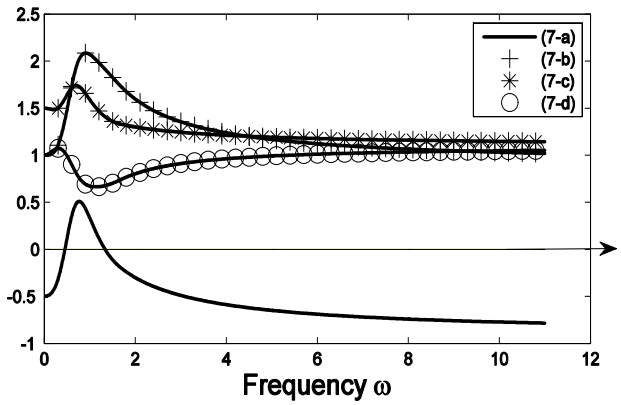

Fig. 4. Identifying the feasible frequency intervals.

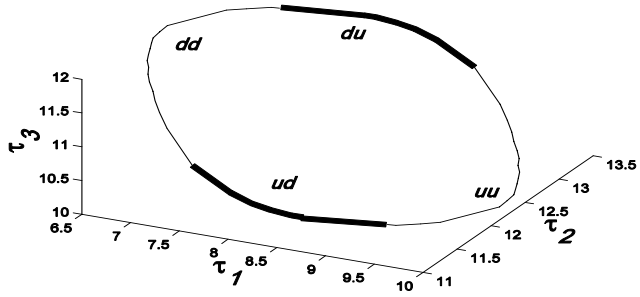

Fig. 5. The four stability crossing curves according to the four cases of Table 2 at ω = 0.49.

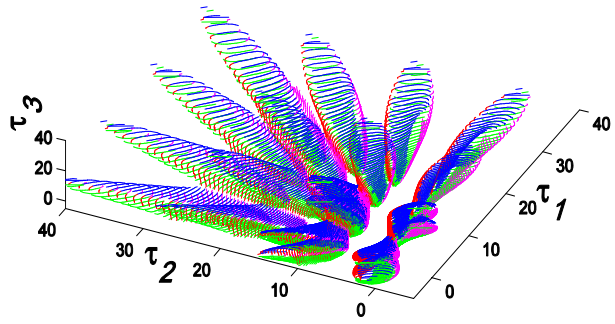

Fig. 6. The stability crossing surfaces.

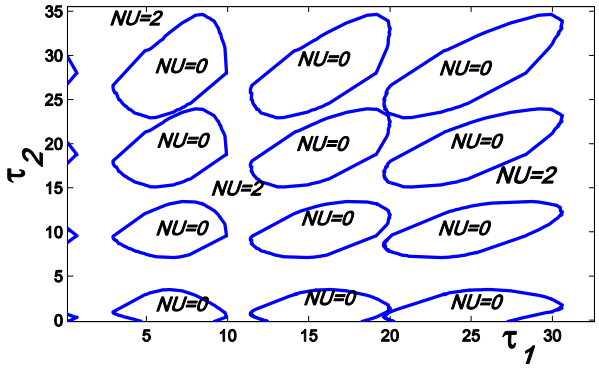

Fig.7. The stability crossing curves at $\tau_3 = 9$ in the τ_1-τ_2 plane.

6. CONCLUSION

In this paper, time-delay systems with three incommensurate delays are considered and the stability crossing surfaces in the three-dimensional space of time delays are identified. The characteristic quasipolynomial of the system is decomposed into the vector sum of four polynomials, and the geometric conditions for forming a quadrangle in the complex plane is used to characterize the stability crossing frequencies and their corresponding points in the time-delay space. Then, different possible stability crossing surfaces are discussed. The algorithm presented in this paper can be used to visualize the stability domains and the stability crossing surfaces in feasible ranges of time delays with a desired precision. The crossing surfaces can be processed and cut in different directions using graphical software such as MATLAB. The extension of the results to the cases where the delays are themselves linear or polynomial functions of several uncertain parameters is of great interest. Also, the derivation of properties of stability crossing surfaces, similar to what obtained in Gu *et al.* (2005) for the stability crossing curves, is promising. The visualization of the stability crossing surfaces for the cases of four or more delays is impossible, however, the quadrangle of quasipolynomial can be replaced by a pentagon, hexagon, etc. for these cases and the stability crossing conditions can be checked numerically (instead of graphical presentation). These subjects can be further investigated.

REFERENCES

Ackermann, J. (2002). *Robust Control: The Parameter Space Approach*, Springer, London.

Barmish, B.R. and Z. Shi (1989). Robust Stability of perturbed Systems with Time Delays, *Automatica*, **25**, 371–381.

Barnett, S. (1983). *Polynomials and Linear Control Systems*. New York, Marcel Dekker.

Bozorg, M. and E.J. Davison (2006). Control of Time Delay Processes with Uncertain Delays: Time Delay Stability Margins. *Journal of Process Control*, **16**, 403-408.

Chen, J., G. Gu and C.N. Nett (1995).A New Method for Computing Delay Margins for Stability of Linear Delay Systems. *Systems and Control Letters*, **26**,107- 117.

Chen, J. and H.A. Latchman (1995) .Frequency Sweeping Tests for Stability Independent of Delay. *IEEE Trans. Auto. Control*, **40**, 1640-1645.

Chiasson, J. N. (1988). A Method for Computing the Interval of Delay Values for Which a Differential-Delay System is Stable. *IEEE Trans. Auto. Control*, **3**, 1176-1178.

Gu, K., V.L. Kharitonov and J.Chen (2003). *Stability of Time-Delay Systems*, Birkhäuser, Boston.

Gu, K., S. Niculescu And J. Chen (2005). On Stability crossing Curves for General Systems with Two Delays. *J. Math. Anal. Appl.*, **311**, 231-253.

Hale, J.K. and W. Huang (1993), Global Geometry of the Stable Regions for Two Delay Differential Equations. *J. Math. Anal. Appl.*, **178**, 344-362.

Niculescu, S.I. (2001). *Delay effects on stability*, Springer-Verlag.

Olgac, N. and R. Sipahi (2002). An Exact Method for the Stability Analysis of Time-Delayed LTI Systems. *IEEE Trans. Auto. Control*, **47**, 793-97.

Rekasius, Z.V. (1980). A Stability Test for Systems with Delays. *Proc. Joint Automatic Control Conf.*, Pap. No. TP9-A.

Richard, J.P. (2003). Time-delay Systems: An Overview of Some Recent Advances and Open Problems. *Automatica*, **39**, 1667-1694.

Sipahi, R. and N. Olgac (2004). A Novel Stability Study on Multiple Time-Delay Systems (MTDS) Using The Root Clustering Paradigm. *Proc. American Control Conference*, **6**, 5422-5427.

Sipahi, R. and N. Olgac (2005). Complete stability robustness of third-order LTI multiple time-delay systems. Automatica, **41**, 1413-1422.

Walton, K.E. and J.E. Marshall (1987). Direct Method for TDS Stability Analysis. *IEE Proceedings,* **134**, 101-107.

Zhong, Q.C. (2006). *Robust Control of Time-Delay Systems,* Springer. London.